Active damping performance of the KAGRA seismic attenuation system prototype

Yoshinori Fujii[1], Takanori Sekiguchi[2], Ryutaro Takahashi[3], Yoichi Aso[3], Mark Barton[3], Fabián Erasmo Peña Arellano[3], Ayaka Shoda[3], Tomotada Akutsu[3], Osamu Miyakawa[2], Masahiro Kamiizumi[2], Hideharu Ishizaki[3], Daisuke Tatsumi[3], Naoatsu Hirata[3], Kazuhiro Hayama[4], Koki Okutomi[3], Takahiro Miyamoto[2], Hideki Ishizuka[2], Riccardo DeSalvo[5] and Raffaele Flaminio[3]

[1]Department of Astronomy, University of Tokyo, Bunkyo, Tokyo 113-0033, Japan
[2]Institute for Cosmic Ray Research, Kashiwanoha, Kashiwa-shi, Chiba 277-8582, Japan
[3]National Astronomical Obsevatory of Japan, Osawa, Mitaka-shi, Tokyo 181-8588, Japan
[4]Osaka City University, Sumiyoshi-ku Sugimoto, Osaka-shi, Osaka 558-8585, Japan
[5]University of Sannio, Corso Garibaldi 107, Benevento 82100, Italy

E-mail: `yoshinori.fujii@nao.ac.jp`

Abstract. The Large-scale Cryogenic Gravitational wave Telescope (formerly LCGT now KAGRA) is presently under construction in Japan. This May we assembled a prototype of the seismic attenuation system for the beam splitter of KAGRA, which we call Type-B and evaluated its performance at NAOJ (Mitaka, Toyko). We tested its frequency performance, active damping performance, vibration isolation performance and long-term stability both in and out of vacuum. From the frequency response test and the active damping performance test, we confirmed that its frequency response was as we designed and that all mechanical resonances which could disturb lock acquisition and observation are damped within the requirement of 1 minute by the active controls.

1. Introduction

KAGRA is a large cryogenic laser interferometric gravitational wave (GW) detector which is being constructed underground at the Kamioka mine in Gifu Prefecture Japan [1]. To prevent the GW signals from being buried in seismic noise, the mirrors of the interferometer are suspended by multi-stage pendulums called the seismic attenuation system (SAS), to prevent seismic motion from transferring to the mirrors and to let the mirrors move as free test masses. By suspending the mirrors, we can attenuate the seismic motion whose resonance frequency is higher than that of the SAS. However, the test mass would still vibrate with large amplitudes at its mechanical resonance frequencies, so in order to lock the interferometer, we have to damp these resonances.

In KAGRA, we use four types of SAS for different tasks: Types A, B, C and Bp. The Type A SAS is an 8-stage pendulum system for the test masses (in the final full configuration which will be used for observation). For the beam splitter and signal recycling mirrors, we will use a 5-stage pendulum system called Type B SAS. The Type C SAS is a 2-stage pendulum system for the mode cleaner mirrors and the Type Bp SAS is used for the power recycling mirrors. In this paper, we report the Type B prototype test. In section 2, we summarize the design of the Type B SAS and its control strategy, and in section 3 the results are described.

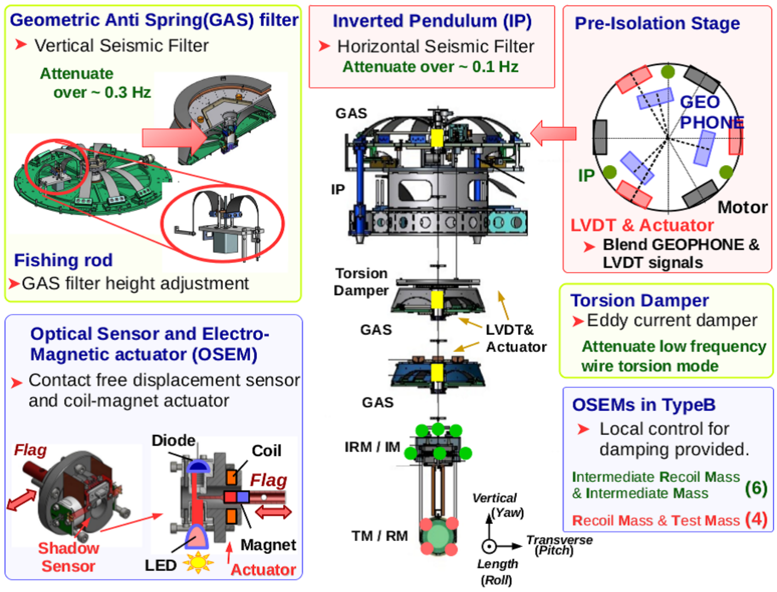

Figure 1. Overview of the Type B SAS for the beam splitter and signal recycling mirrors. The yellow boxes in the center show the position of the LVDTs and the actuators, while the red and green dots show the position of the OSEMs. We can actuate the top stage in 3 DoF, each GAS filter in the vertical direction, the IM for all 6 DoF, and the TM in 3 DoF.

2. Type B SAS

2.1. Mechanical details

The mechanical components of the Type B SAS are as follows (see also Figure 1);

- Inverted Pendulum (IP): three inverted pendulum legs support the SAS, and work as a horizontal seismic filter whose resonance frequency can tuned as low as 0.1 Hz. The IP can damp not only the micro seismic motion at around 0.2 Hz, but also the multi-stage pendulum resonances around 1 Hz.
- Geometric Anti-Spring (GAS) filters: each filter is a vertical seismic isolator whose resonance frequency is tuned around 0.3 Hz. Each GAS filter consists of a set of curved maraging steel blades and has a spring height adjustment attained through a motorised blade with low stiffness set in parallel to the GAS springs, called a fishing rod. The fishing rod can compensate weight of a few hundred grams. Type B SAS has three GAS filters.
- Torsion Damper: a non-contacting damper placed above the middle GAS filter, which damps low-frequency wire torsion modes of the SAS using eddy current damping.
- Payload: a 2-stage, 4-mass pendulum consisting of the intermediate recoil mass (IRM), intermediate mass (IM), recoil mass (RM) and test mass (TM). We can adjust the tilt of the TM and RM by applying forces on the TM from the RM.

Each component has sensors and actuators: The IP has three each of coil-magnet actuators and two kinds of sensors arranged in a triangle. Linear variable differential transformers (LVDTs) are used at low frequencies and geophones are used at high frequencies, with a crossover around 50 mHz. Each GAS filter has an LVDT as a vertical displacement sensor and a coil-magnet actuator. The payload is equipped with Optical Sensor and Electro-Magnetic actuator (OSEM) units [2] (see Figure 1), which combine a shadow sensor and a coil-magnet actuator. The available range of the OSEMs is wide (1 mm), although the coupling noise is large. By using 6 OSEMs on the IM and IRM, and 4 OSEMs on RM and TM, we can sense and actuate the relative motion of the IRM and IM, and the RM and TM. The signals from those sensors are mainly used to compensate thermal drifts and to damp the resonances.

2.2. Local active control strategy

Active damping controls are required to suppress the motion caused by the external disturbance driving the mechanical resonances of the SAS. The control system is set up to progress through the following states of operation: (a) damping, (b) lock acquisition and (c) observation [2]. The purpose of the damping state is purely to reduce large-amplitude motion at the mechanical resonances due to external disturbances. In this state the active controls are required to minimize the decay time of the SAS to allow fast recovery to the observation state. We have set a goal for the required damping time of 1 min. In the lock acquisition state the speed of the mirrors has to be suppressed to allow the mirrors to be trapped into the linear range of the interferometer signals. The control noise must be designed not to increase the RMS of linear speed of each suspended mirror. To lock the optical cavities, the RMS velocities and the angular fluctuations of the mirrors are typically required to be less than 1 μm/sec and a few μrad respectively [3]. After lock acquisition is achieved, we enter the observation state, in which the interferometer operates. In each state, we use different control system, for example, OSEMs are used only in the damping and lock acquisition states because of their large noise coupling. Conversely, geophones are used beginning with the lock acquisition state due to their small range.

3. Performance test of type B SAS prototype

After assembling the Type B SAS prototype, we constructed a servo system for damping (see Figure 2) and conducted performance tests of the prototype: frequency response, active damping performance, vibration isolation performance and long term stability performance. In these tests, an optical lever was set at the back side of the TM to sense its angular motion. In this section the measured frequency response and active damping performance are summarized.

3.1. Frequency response

To confirm the SAS works as designed we measured transfer functions from actuators to sensors of each of the components and compared them with results from a rigid-body simulation [4]. The transfer functions were measured for all the 15 degrees of freedom (DoFs) that we can actuate, in air and with the controls switched off. A typical result is shown in Figure 3, where the blue and red lines show the simulated and measured results. The simulation tool [4] drove the tests and allowed to debug the system.

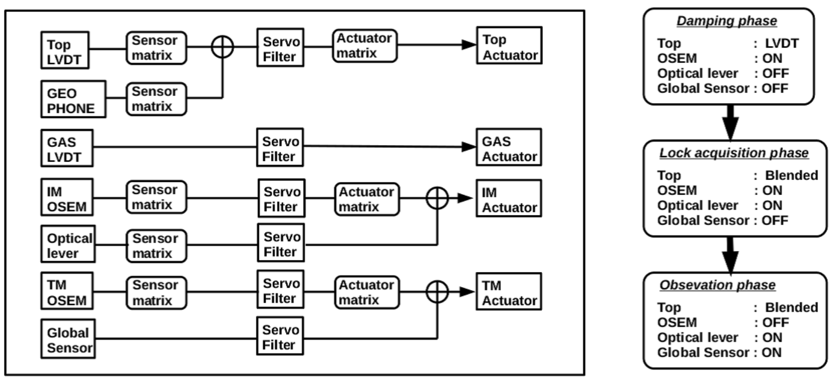

Figure 2. Left: local damping control for performance test of the type B SAS prototype. Signals from photo sensors are used instead of as-yet unavailable main interferometer signals. Right: local control transition toward observation state.

3.2. Active damping performance in damping state

To test if the mechanical resonances of the SAS were damped within the requirement of 1 min by the active controls in the damping state, we measured the $1/e$ damping time with the controls on and off. Although one mode was slow to damp, we found we could damp within 1 min all the resonances which were likely to disturb lock acquisition and observation. In this measurement, we obtained the damping time of the mechanical resonances by exciting the system with a virtual actuator and measuring decay signals from virtual sensors [2]. Also, only modes with resonance frequencies below 20 Hz were measured because of the difficulty in exciting the system above 20 Hz with actuators on the SAS. According to the results shown in Figure 4, the longest damping time without control is around 20 min, but this is reduced to 3 min with control. For only one resonance at 0.6 Hz we could not reduce the decay time below 1 min, however, this resonance is hard to excite other than by external disturbance. The mode is concerning with transversal motions of TM and RM. Even if it becomes excited, it cannot affect the lock acquisition unless the amplitude is extremely large, such as 1 mm, which is the requirement of the beam spot fluctuation on the optics of the interferometer.

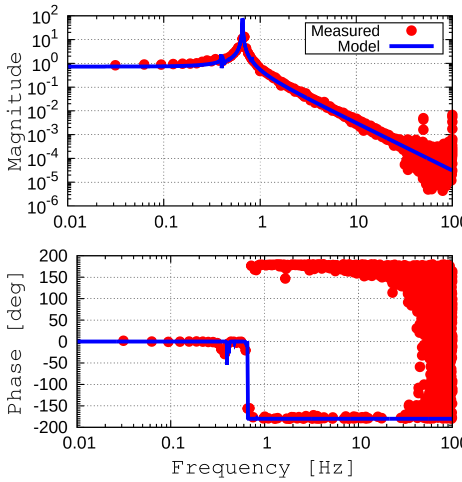

Figure 3. Transfer function of the TM Length DoF in the air

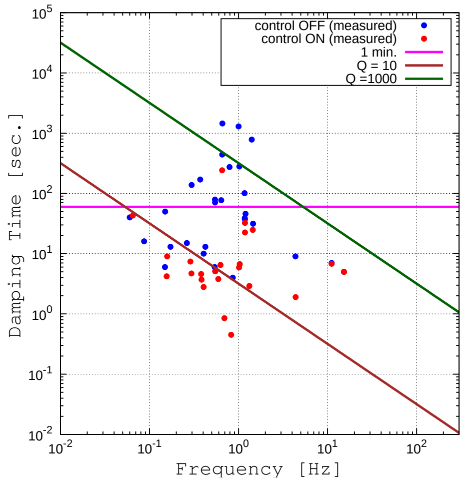

Figure 4. Active damping performance of the prototype

4. Summary

We assembled one whole Type B SAS prototype and evaluated its performance. From the frequency response test, we confirmed all the components of the SAS were properly suspended. Also, from the active damping performance test, we confirmed we were able to damp the mechanical resonances caused by external disturbances and start observation again within a few minutes.

Acknowledgments

This work was supported by MEXT, JSPS Leading-edge Research Infrastructure Program, JSPS Grant-in-Aid for Specially Promoted Research 26000005, MEXT Grant-in-Aid for Scientific Research on Innovative Areas 24103005, JSPS Core-to-Core Program, A. Advanced Research Networks, and the joint research program of the Institute for Cosmic Ray Research, University of Tokyo, and JSPS Grant-in-Aid for JSPS Fellows 15J11064, 14J10236. We thank personnel of the Advanced Technology Center of the National Astronomical Observatory of Japan for providing items of equipment for our experiments.

References

[1] Aso Y, et al. 2013, Physics Review D 88 043007
[2] Sekiguchi T, 2016, Ph.D thesis
[3] Michimura Y, 2012, JGW document JGW-T1202403-v1
[4] Sekiguchi T, 2012, Master's thesis